

## Solution Properties of a Novel Ampholytic Polyphenylene Sulfide

Hui Xiao, Rong Tao, Wei Cui, Shuai Zhang, Rui Hai Li

Department of Polymer Science and Engineering, Sichuan University, Chengdu 610065, China

Correspondence to: H. Xiao (E-mail: xhdgjgjfz@hotmail.com)

**ABSTRACT:** A polyampholyte was prepared from polyphenylene sulfide (PPS) by sulfonation, followed by bromination, and then the substitution of bromine by a quaternary ammonium group and tertiary amine group. The aqueous solution properties of the polyelectrolyte and polyampholyte with different ionic groups were investigated by viscometric measurement and rheological behavior measurement. The results show that the viscosities of the polyelectrolyte and polyampholyte were not only dependent on the nature of acid and base substituents along the polymer chain but also on the external factors, such as pH and small-molecule electrolytes. In pure water, the rheological behavior of the polyelectrolyte showed an obvious critical shear rate in this circumstance; the polyampholyte showed a relatively stable shear rate compared with the polyelectrolyte. However, in salt-saturated water, the viscosity decreased quickly with increasing shear rate. © 2012 Wiley Periodicals, Inc. *J. Appl. Polym. Sci.* 000: 000–000, 2012

**KEYWORDS:** polymer rheology; polymer synthesis and characterization; structure—property relations

Received 17 October 2011; accepted 10 January 2012; published online

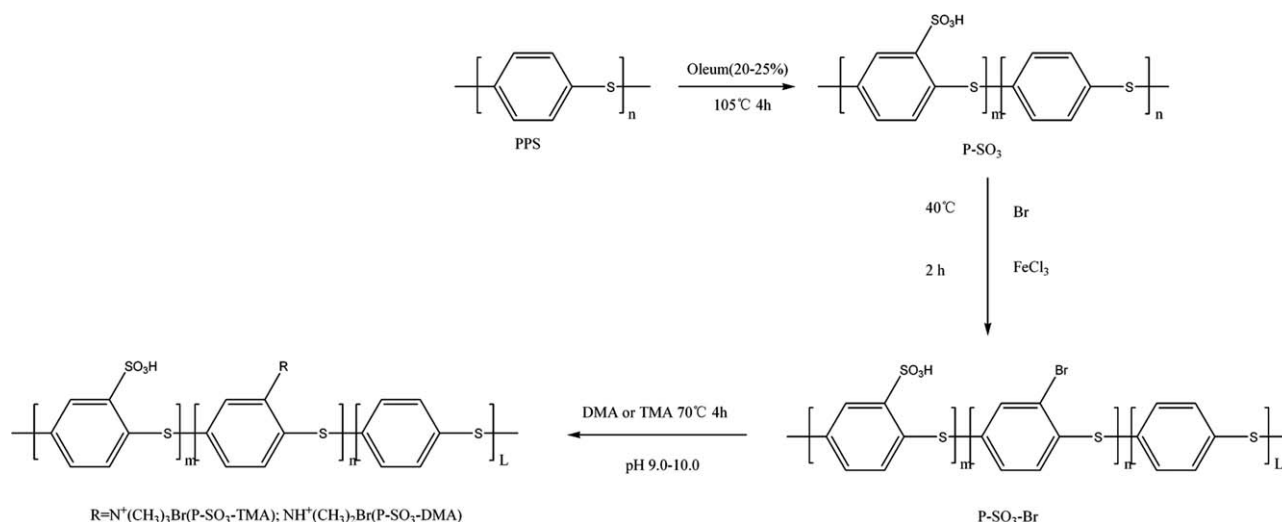
DOI: 10.1002/app.36809

### INTRODUCTION

Polyampholytes, a kind of charged polymer with both anionic and cationic groups on its polymer chain, has attracted much attention because of their unique structures and excellent properties in recent years.<sup>1–4</sup> Compared with polyelectrolytes, electrostatic interactions in polyampholytes exhibit both electrostatic repulsion and electrostatic attraction.<sup>5</sup> The electrostatic interactions are influenced by internal factors (e.g., the nature and distribution of the acid and basic substituents, hydrophobicity) and external factors (e.g., pH, temperature, ionic strength of the solution, thermodynamic quality of the solvents). The existence of the isoelectric point (IEP) and the antipolyelectrolyte effect are unique properties of polyampholytes. At the IEP, there are equal numbers of positive and negative charges along the polymer chain; this gives it a net charge of zero.<sup>6</sup> The *antipolyelectrolyte effect* refers to the polymer chain expansion at the IEP due to the addition of small-molecule electrolytes, such as NaCl, CaCl<sub>2</sub>, and MgCl<sub>2</sub>.<sup>7</sup> Since the first study on the synthesis of polyampholytes in the 1950s by Alfrey et al.,<sup>8</sup> a number of investigations have focused on the unusual properties of polyampholytes.<sup>9–13</sup> These polyampholytes are mostly synthesized by zwitterionic monomers, such as sulfobetaines and carboxybetaines. The preparation, characterization, and application of zwitterionic organic polymers (or polymeric betaines) have been reviewed by many researchers.<sup>2,14</sup> Because of previously mentioned polyampholytic characterization and

unique salt-responsive behavior,<sup>2,15</sup> they have been widely proposed for various industrial applications, such as multifunctional drilling-fluid additives,<sup>16–18</sup> salt-resistant thickeners,<sup>19</sup> fracturing additives,<sup>20</sup> cementing extra-agents,<sup>21</sup> and biomaterials to prevent postsurgical adhesions. Meanwhile, in the application of drilling-fluid additives, with increasing depth of the well, the polyampholyte are in demand to work at more elevated temperature and pressures. The synthesis and aqueous solution properties of these betaine-type polyampholytes have been reported by several authors, including Michael J. Fevola et al.,<sup>22</sup> Nelly and Andren,<sup>23</sup> Ali and Rasheed,<sup>24</sup> Lee and Huang,<sup>25</sup> Zheng et al.,<sup>26</sup> and Kudaibergenov and coworkers.<sup>27,28</sup> Although there have also been some studies on polyampholytes with acid groups and basic groups on different chain units<sup>29,30</sup> and synthesis and hydrolysis to obtain polyampholytes, few studies have been done on the aqueous solution properties of polyampholytes with semirigid backbones and random distribution of cations and anions along the polymer chain. Until now, a convenient and effective method for obtaining new types of polymer, in which the polyampholyte is obtained by postfunctionalization of the commercialized polymer, have rarely been reported. There are only a few reports<sup>31–33</sup> in the literature on the rheological behaviors of polyelectrolytes and their corresponding polyampholytes.

In this study, the synthesized route of polyampholytes was initiated with the sulfonation of phenyl groups, followed by



**Scheme 1.** Preparation of P-SO<sub>3</sub>, P-SO<sub>3</sub>-Br, P-SO<sub>3</sub>-TMA, and P-SO<sub>3</sub>-DMA.

bromination, and the substitution of bromine by quaternary ammonium groups and tertiary amine groups.<sup>34</sup> The study was an interesting opportunity to examine the aqueous solution properties of polyelectrolytes and their corresponding polyampholytes with the same number of anionic groups as the polyelectrolytes. Furthermore, the solution properties of different kinds of cationic groups along the polymer chain were also studied.

## EXPERIMENTAL

### Materials

Polyphenylene sulfide (PPS) was provided by Sichuan De Yang Science and Technology Co., Ltd., China. PPS was cleaned with acetone, dried *in vacuo* (70°C) to a constant weight, and then ground by a disintegrator to obtain homogeneous small particles (<1 mm). Oleum (20–25%), acetone, ether absolute, absolute ethanol, bromine, ferric chloride (FeCl<sub>3</sub>), sodium hydroxide (NaOH), hydrochloric acid (HCl), dimethylamine (DMA), and trimethylamine (TMA) were purchased from Chengdu Kelong Chemical Regents Factory, China (analytical grade). Deionized (DI) water (electrical resistance = 18 M) was used. Dimethyl sulfoxide (DMSO) was purchased from Tianjin Damao Chemical Reagent Factory, China. The reagent-grade salts KBr, NaCl, NH<sub>4</sub>Cl, CaCl<sub>2</sub>, MgCl<sub>2</sub>, KI, KCl, and LiCl were purchased from Chengdu Kelong Chemical Regents Factory.

### Preparation of the Sulfonated Polyphenylene Sulfide (P-SO<sub>3</sub>)

The sulfonation of PPS was carried out according to a procedure previously described in the literature.<sup>35,36</sup> P-SO<sub>3</sub> was synthesized via an electrophilic aromatic substitution reaction. PPS was dissolved in oleum (20–25%) to form a 1 g/15 mL solution. The solution was made by vigorous stirring in a three-necked flask with a sealed mechanical stirrer, a drying tube, and a thermometer. The flask was put in a thermostated oil bath. The reaction mixture became a dark brown slimelike substance when oleum was poured into the flask at room temperature. With stirring and an elevated temperature of 105°C, the mixture gradually dissolved in the oleum to form a dark brown solution. The reaction time was 4 h. Subsequently, the polymer solution

was added dropwise to a nonsolvent bath of ether to remove a majority of the oleum. The dark polymer was then separated by filtration, vigorously washed with acetone, and further purified by a Soxhlet extractor for 48 h. Finally, P-SO<sub>3</sub> was dried in a vacuum oven (Beijing Zhongxingweiye Co., Ltd., China) for 48 h at 80°C for the complete removal of the solvent.

The structure of P-SO<sub>3</sub> is shown in Scheme 1.

### Preparation of the Bromated Sulfonated Polyphenylene Sulfide (P-SO<sub>3</sub>-Br) and Amphoteric PPS (P-SO<sub>3</sub>-DMA and P-SO<sub>3</sub>-TMA)

Amounts of 10 g of P-SO<sub>3</sub>, 100 mL of DMSO, and 0.4 g (4%) FeCl<sub>3</sub> were added to a 250-mL dried three-necked flask, which was equipped with a mechanical stirrer, condenser pipe, drying tube, and atmospheric dropping funnel. Then, the mixture, under N<sub>2</sub>, was stirred and heated at 40°C to form a homogeneous solution. The bromine solution (2.5 mL of bromine was diluted in 75 mL of DMSO) was dropped into the flask for 0.5 h with mechanical stirring and subsequently heated to 40°C for 2 h. We sampled 10 mL of the solution to purify and check the structure of P-SO<sub>3</sub>-Br. We then adjusted the pH to 9.0–10.0 and divided the residual solution into two 250-mL, three-necked flasks. DMA solution (3.5 mL of 33% DMA solution diluted in 35 mL of ethanol) and TMA solution (6.5 mL of 33% TMA solution diluted in 65 mL of ethanol) were, respectively, dropped into the three-necked flasks for 30 min at 40°C. The temperature was elevated to 70 or 80°C for 4 h. With the reaction, the amphoteric PPS was gradually precipitated from the solution in the reaction because DMSO was a poor solvent for the amphoteric polymer. After reaction was complete, the product was diluted, washed by the addition of ethanol, and separated by filtration (the original solution was so viscous that it was difficult to filtrate the solution directly). Subsequently, the precipitation was purified by ethanol to remove anionic polymer and further purified by the Soxhlet extractor for 48 h. The purified product was dried at 80°C *in vacuo* to a constant weight.

The structure of P-SO<sub>3</sub>-Br is shown in Scheme 1. Bromination is also an electrophilic substitution reaction. However,

because of the strong electronegativity, bromine can largely decrease the electronic cloud density of the benzene ring. Furthermore, there were large steric effects when the bromine was added to the polymer, so the possibility of further bromination could be neglected. Also, the sulfonic group is a special kind of electron-withdrawing group, so it can largely decrease the cloud density of the benzene ring, and bromination occurred on the same benzene ring where sulfonation could essentially be excluded.

### Characterization

**Fourier Transform Infrared (FTIR) Measurements.** The FTIR spectra were recorded with a Nicolet-560 spectrophotometer (USA) in the range 400–4000  $\text{cm}^{-1}$ . The absorption spectra of P-SO<sub>3</sub>, P-SO<sub>3</sub>-Br, P-SO<sub>3</sub>-TMA, and P-SO<sub>3</sub>-DMA were measured in KBr pellets.

**IEP Measurements.** IEPs were tested by a nanoparticle size and potential analyzer (Malvern Instrument Co., Ltd, UK) (Nano-ZS; test temperature = 25.0°C). The IEPs of P-SO<sub>3</sub>-TMA and P-SO<sub>3</sub>-DMA were measured in different pH aqueous solutions.

**Measurement of the Degree of Sulfonation (DS) of P-SO<sub>3</sub>.** The DS of P-SO<sub>3</sub> was the number of sulfonic acid groups per repeating unit along the polymer chain. It was determined by titration with 0.01M NaOH (aqueous). In a typical experiment, 0.1 g of P-SO<sub>3</sub> was added to 25 mL of DI water as a titrated solution. Then, the DS was calculated according to the volume of NaOH solution. The formula for calculating DS was as follows:

$$DS = \frac{M_{PPS} C_{NaOH} V_{NaOH}}{m_{P-SO_3} - 80 C_{NaOH} V_{NaOH}}$$

where  $M_{PPS}$  is the average molecular weight of the repeating unit of PPS, which is 108 g/mol,  $m_{P-SO_3}$  is the quantity of P-SO<sub>3</sub> (g), and  $C_{NaOH}$  and  $V_{NaOH}$  refer to the concentration of NaOH (mol/L) and the titration volume (L), respectively.

**Determination of the Bromine Content by the Mohr Method.** The bromine content in the polymer was measured by Mohr Method. First, the bromine in the polymer was converted to bromonium ions by oxygen flask combustion. NaOH (0.5M, aqueous), DI water, and 33% hydrogen peroxide (volume ratio = 9: 10:1) were used as an absorbing solution. After complete absorption, the solution was shifted to a 100-mL conical flask. The solution was boiled for 6 min to remove the residual hydrogen peroxide and to convert  $S^{2-}$  into  $SO_4^{2-}$  and then cooled to room temperature. Second, the bromine content was measured by precipitation titration of the Mohr method. AgNO<sub>3</sub> (0.01M) was prepared and standardized against a NaCl solution. Reagent-grade NaCl was dried for 4–5 h at 300–400°C. An amount of 2 mL of a 5% K<sub>2</sub>CrO<sub>7</sub> solution was added to the solution as an indicator and subsequently titrated with 0.01M AgNO<sub>3</sub> from yellow to pink. The Mohr measure was conducted under a pH of 6.5–8. An indicator blank was also measured by a small amount of potassium bromide in 100 mL of the boiled absorbing solution containing 2 mL of a 5% K<sub>2</sub>CrO<sub>7</sub> solution. The formula for calculating the bromine content ( $M_{Br}$ ) follows:

$$M_{Br} = 79.9 \text{ g/mol}$$

$$\%Br = \frac{79.9 C_{AgNO_3} V_{AgNO_3}}{m} \times 100\%$$

where  $m$  is the mass of the polymer sample,  $C_{AgNO_3}$  is the concentration of AgNO<sub>3</sub> solution (mol/mL), and  $V_{AgNO_3}$  is the titration volume of AgNO<sub>3</sub> (mL).

The bromine content was calculated by the bromine degree ( $D_b$ ), which is the number of Br per repeating unit along the polymer chain. However, the calculation was approximate because of the uncertainty of the number of sulfonic acid groups and Br per repeating units. The formula for calculating  $D_b$  is as follows:

$$D_b = \frac{M C_{AgNO_3} V_{AgNO_3}}{m - m_{SO_3} m_{Br}} \times 100\%$$

where  $M$  is the average molecular weight of the repeating unit of PPS, which is 108 g/mol,  $m_{SO_3}$  is the mass of the sulfonic acid group, and  $m_{Br}$  is the mass of bromine.

**Viscometric Measurements.** Viscometric measurements were carried out with an Ubbelohde viscometer (Shanghai Shengyi Glass Co., Ltd., China) (flow time = 136.79 s for pure water) at  $30 \pm 0.1^\circ\text{C}$ . The polymer samples were dissolved in electrolyte solutions of different cation types, anion types, and concentrations to obtain stock solutions of approximately 1 g of polymer per 100 mL of solvent (0.004 mol of SO<sub>3</sub><sup>-</sup> and 0.0026 mol of positively charged group per 100 mL). The specific viscosity ( $\eta_{sp}$ ) was calculated as follows:

$$\eta_{sp} = \frac{t - t_0}{t_0}$$

where  $t_0$  is the flow time of solvent (DI water) and  $t$  is the flow time of the polymer solution. The reduced viscosity was calculated by the division of  $\eta_{sp}$  by concentration of solution ( $c$ ) (g/mL). The determinations of  $t$  and  $t_0$  were confined to  $\pm 2\%$ .

**Rheological Behavior Measurements.** Solutions (0.5 g/dL) of P-SO<sub>3</sub>, P-SO<sub>3</sub>-TMA, and P-SO<sub>3</sub>-DMA were prepared for rheological behavior measurement. The rheological behavior measurements were carried out on a Malvern Gemini Rheometer (Malvern Instruments, United Kingdom). A cone-and-plate geometry of CP40/4 (cone angle = 4°, cone radius = 40 mm) was used as the measurement system. The gap between the cone and the plate was adjusted to 0.15 mm. All of the rheological behavior measurements were performed at  $30 \pm 0.1^\circ\text{C}$ . In this study, the shear-rate-dependent measurements of the viscosity were found in the range 0.01–100 1/s.

## RESULTS AND DISCUSSION

### P-SO<sub>3</sub> Synthesis

The synthesis of P-SO<sub>3</sub> was carried out with oleum as the sulfonating agent at different ratios of sulfonating agent, temperatures, and times. The corresponding DSs are shown in Table I.

The results in Table I indicate that DS was dependent on the sulfonating agent, temperature, and time. For a 10 g/150 mL ratio of PPS to fuming sulfuric acid, DS of the polymer was 47.6% at 105°C for 4 h; this was equivalent to a little fewer

**Table I.** Synthesis of the P-SO<sub>3</sub>

$M^{\text{PPS}}$ (g) <sup>a</sup>	$K^{\text{oleum}}$ (mL) <sup>b</sup>	$M^{\text{PPS}}/K^{\text{oleum}}$	t (h)	Temperature (°C)	DS (%) <sup>a</sup>
10	70	1: 7	4	105	—
10	100	1: 10	4	105	40.6
10	150	1: 15	4	105	47.6
10	200	1: 20	4	105	47.6
10	150	1: 15	4	80	33.2
10	150	1: 15	4	100	42.0
10	150	1: 15	0.5	105	39.2
10	150	1: 15	2	105	45.7

$M^{\text{PPS}}$ , weight of PPS in the reaction;  $K^{\text{oleum}}$ , volume of oleum in the reaction.

<sup>a</sup>DS obtained by titration.

than half of the aromatic rings having been sulfonated and nearly half of the aromatic rings still available for bromination on the polymer chain.

#### P-SO<sub>3</sub>-Br, P-SO<sub>3</sub>-DMA, and P-SO<sub>3</sub>-TMA Synthesis

P-SO<sub>3</sub>-Br was prepared with Br<sub>2</sub> as the bromide reagent and FeCl<sub>3</sub> as the catalyst. The bromine contents of P-SO<sub>3</sub>-Br at different ratios of catalyst, times, and temperatures are shown in Table II. As was evident, an excellent  $D_b$  (35.25%) was obtained under the optimum reaction conditions (4% catalyst, 40°C, and 4 h). Namely, the number of bromine groups was equivalent to 59% of the sulfonic acid groups along the polymer chain.

The bromine content of polyampholyte was also examined by the Mohr method. The results show that bromine was completely substituted by quaternary ammonium groups under the reaction conditions of a 1: 1.2 ratio of P-SO<sub>3</sub>-Br to the volume of TMA, 70°C, and 4 h and by tertiary amine groups at a 1: 1.2 ratio of P-SO<sub>3</sub>-Br to the volume of DMA, 80°C, and 4 h, as shown in Tables III and IV, respectively.

#### Structural Characterization

Figure 1(a) shows the FTIR spectra of P-SO<sub>3</sub>. The absorption bands at 1230, 1188, and 1034 cm<sup>-1</sup> were ascribed to asymmet-

**Table II.** Synthesis of the Bromide Sulfonated Polyphenylene Sulfide (P-SO<sub>3</sub>-Br)

$M^{\text{SPPS}}$ (g)	$K^{\text{FeCl}_3}$ (%)	t (h)	Temperature (°C)	Bromine content (%)	$D_b$ (%)
5	3	4	40	0.2369	31.99
5	4	4	40	0.2596	35.05
5	5	4	40	0.2612	35.25
5	4	3	40	0.2512	33.91
5	4	5	40	0.2599	35.09
5	4	4	30	0.2486	33.56
5	4	4	50	0.2603	35.14

$M^{\text{SPPS}}$ , weight of P-SO<sub>3</sub> in the reaction;  $K^{\text{FeCl}_3}$ , mass fraction of catalyst in the reaction.

**Table III.** Influencing Factors on the Quaternary Ammonium

Number	$M^{\text{P-SO}_3\text{-Br}}/K$ (g/mL)	Temperature (°C)	t (h)	$D_b$ (%)
1	1: 0.5	40	2	~5.6
2	1: 0.5	40	4	~4.3
3	1: 0.6	50	4	~3.1
4	1: 0.8	60	3	~2.9
5	1: 1	70	3	~1.1
6	1: 1.2	70	4	~0

$M^{\text{P-SO}_3\text{-Br}}$ , weight of P-SO<sub>3</sub>-Br in the reaction; K, volume of TMA.

ric and symmetric O=S=O stretching vibrations of sulfonic acid groups.<sup>34</sup> The S-O stretching of the sulfonic acid groups was at 690 cm<sup>-1</sup>. The bands at 890 and 811 cm<sup>-1</sup> were attributed to the benzene ring with three replaced groups instead of two replaced groups. The absorption at 3427 cm<sup>-1</sup> revealed the existence of the stretching vibration of -OH or the absorbed water of sulfonic acid groups. The spectra of P-SO<sub>3</sub>-Br showed a significant band (at 939 cm<sup>-1</sup>), as shown in Figure 1(b), which was attributed to the spectra of the characteristic frequency of benzene halide. The peaks at 2850–2970 and 1477 cm<sup>-1</sup> in Figure 1(c,d) represent the asymmetrical stretching vibration and stretching vibration of methyl, respectively.<sup>37</sup> The wide peak at 3000–3250 cm<sup>-1</sup> in Figure 1(d) is the stretching vibration of the N-H bond.<sup>38</sup> These observations confirmed the successful chemical modification of P-SO<sub>3</sub>, P-SO<sub>3</sub>-Br, P-SO<sub>3</sub>-TMA, and P-SO<sub>3</sub>-DMA.

#### Properties of the Polyelectrolyte and Polyampholyte

**Solubility Measurements.** The pH of the P-SO<sub>3</sub> solution with a concentration of 2% was 2.3, the pH of P-SO<sub>3</sub>-TMA was 8.1, and that of P-SO<sub>3</sub>-DMA was 6.4. The solubility behavior of the polymers is shown in Table V. The polyelectrolyte was found to be soluble in most polar solvents, such as water, methanol, and ethanol, but was only slightly soluble in tetrahydrofuran. Unlike in most studies,<sup>36,39</sup> the polyampholyte was found to be soluble in water. The solubility behavior of the polyampholyte (at the IEP) in this study could be interpreted by the big steric hindrance between the positive and negative charges along the main chain. Furthermore, the polyampholyte was also found to be insoluble in most polar solvents.

**Table IV.** Influencing Factors on the Tertiary Amine

Number	$M^{\text{P-SO}_3\text{-Br}}/K'$ (g/mL)	Temperature (°C)	t (h)	$D_b$ (%)
1	1: 0.5	40	2	~6.1
2	1: 0.5	40	4	~5.5
3	1: 0.6	50	4	~4.6
4	1: 0.6	60	3	~3.8
5	1: 1	70	3	~2.3
6	1: 1.2	70	4	~1.0
7	1: 1.2	80	4	~0

$M^{\text{P-SO}_3\text{-Br}}$ , weight of P-SO<sub>3</sub>-Br in the reaction; K', volume of DMA.

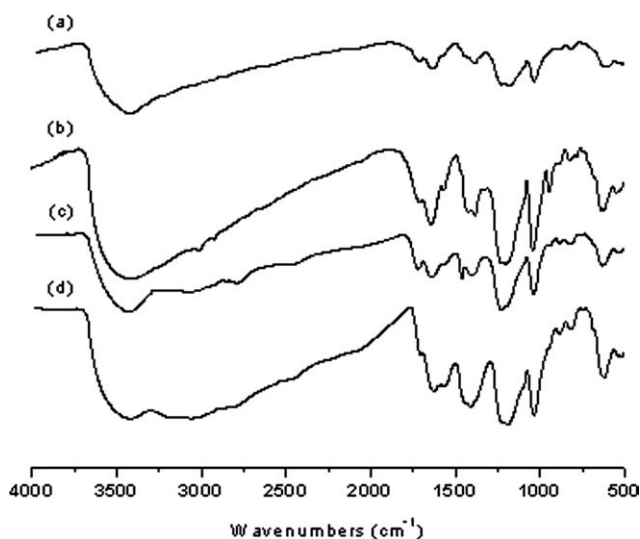


**Figure 1.** FTIR spectra of (a) P-SO<sub>3</sub>, (b) P-SO<sub>3</sub>-Br, (c) P-SO<sub>3</sub>-TMA, and (d) P-SO<sub>3</sub>-DMA.

**Influence of pH on the Reduced Viscosity of the Polyelectrolyte and Polyampholyte in Pure Water.** Figure 2 represents the effect of the pH on the reduced viscosity of P-SO<sub>3</sub>, P-SO<sub>3</sub>-TMA, and P-SO<sub>3</sub>-DMA in pure water. The adjustment of the pH was achieved via the addition microliter aliquots of NaOH or HCl. The pH of the solution was measured by a PB-10 pH meter. In the absence of electrolytes, the conformations of the polyelectrolyte and polyampholyte were sensitive to pH because the electrostatic interaction was operative under these conditions because of the lack of charge screening. At low pH, the sulfonic acid groups were shielded by exceed H<sup>+</sup>; this led to weak repulsive forces, so the polymer coiled to contract. With increasing pH, the electrostatic repulsions of the negative charge increased, and this led to extended conformations and large hydrodynamic volume conformations of P-SO<sub>3</sub>. This was consistent with previous reports.<sup>22</sup> However, at high pH, the hydrodynamic volume and solution viscosity of P-SO<sub>3</sub> decreased slightly. This effect was attributed to the charge screen of Na<sup>+</sup> to the repulsive forces of the sulfonic acid groups.<sup>24</sup> In this case, the polyampholyte showed the behavior of the polyelectrolyte

**Table V.** Solubility of P-SO<sub>3</sub> and the Corresponding Polyampholytes of P-SO<sub>3</sub>-TMA and P-SO<sub>3</sub>-DMA

Solvent	Polarity index	Solubility		
		P-SO <sub>3</sub>	P-SO <sub>3</sub> -DMA	P-SO <sub>3</sub> -TMA
Water	10.2	+	+	+
Methanol	6.60	+	-	-
Ethanol	4.30	+	-	-
DMSO	7.20	+	±	±
Tetrahydrofuran	4.20	±	±	±
Dimethylacetamide	6.40	+	±	±

+, soluble; -, insoluble; ±, partially soluble. A solution of 2% w/w was made after we heated the solution at 70°C for 1 h and then cooled it to room temperature.

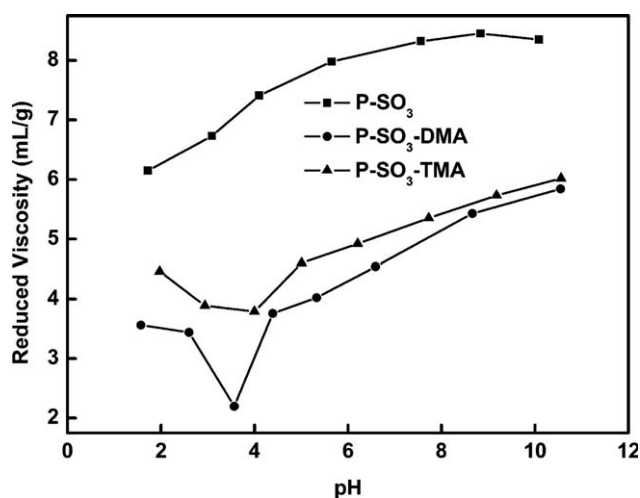


**Figure 2.** Dependence of the reduced viscosity on pH in a dilute solution (0.01 g/mL) of polyelectrolyte (P-SO<sub>3</sub>) and polyampholyte (P-SO<sub>3</sub>-DMA and P-SO<sub>3</sub>-TMA).

because of the suppression of ionization of the tertiary amine group and the shielding of repulsion among the quaternary amine groups. With decreasing pH, the enhanced ionization of tertiary amine groups and quaternary amine group compensated for the sulfonic acid groups and, thus, relieved the repulsive forces among the sulfonic acid groups. A minimum viscosity was observed when the polyampholytes became charge-balanced polyampholytes, as shown in Figure 2.

As shown in Figure 2, the reduced viscosities of P-SO<sub>3</sub>-TMA were larger than those of P-SO<sub>3</sub>-DMA. At pH 4, there existed a minimum reduced viscosity because of the conformation; this allowed the highest degree of cation/anion pairing and minimal hydration of the associated mer units.<sup>6</sup> Also, the curve of P-SO<sub>3</sub>-TMA had merely a slowly decreasing trend. This was because of the strong alkalinity of the quaternary amine groups and the alkalescence of the tertiary amine groups. In the solutions, the alkalinity of the quaternary amine groups formed loose cation/anion pairing; however, the alkalescence of the tertiary amine groups may have led to compact cation/anion pairing. As a result, the attractive interactions between charges of P-SO<sub>3</sub>-DMA were much stronger than those of P-SO<sub>3</sub>-TMA, so the hydrodynamic volume of P-SO<sub>3</sub>-DMA was much smaller. Furthermore, the stronger attractive interactions of P-SO<sub>3</sub>-DMA led to much larger compression comparing with P-SO<sub>3</sub>-TMA.

**Viscosity Behavior of the Polymers in Aqueous and Aqueous Salt Solutions.** Figure 3 shows the viscosity behavior of the polymer with different concentrations. The typical polyelectrolyte characteristic were shown in the curve with the concavity of P-SO<sub>3</sub>. This could be explained by the different conformations of P-SO<sub>3</sub> in different concentrations in DI water. With dilution, the polyelectrolyte gradually shifted from a coil-like conformation with small hydrodynamic volume to a rodlike conformation with large hydrodynamic volume in the solution; this was aroused by the electrostatic repulsion of negative charges along the chain that arose from the dissociation of

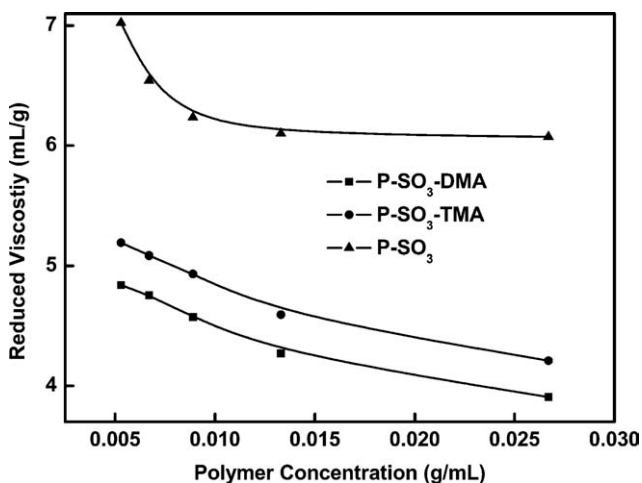


**Figure 3.** Influence of the polymer concentration on the reduced viscosities of P-SO<sub>3</sub> at pH 2.3, P-SO<sub>3</sub>-TMA at pH 8.1 ( $\text{PH}_{\text{IEP}} = 4.08$ ), and P-SO<sub>3</sub>-DMA at pH 6.5 ( $\text{PH}_{\text{IEP}} = 3.84$ ).  $\text{PH}_{\text{IEP}}$  PH of isoelectric point.

polyelectrolyte in the ionizing solvent (e.g., water). The counterions separated from the chain in dilute solution to leave the negative charges behind and, thus, with dilution, further lead to separation. On the other hand, the tendencies of the curves of P-SO<sub>3</sub>-TMA and P-SO<sub>3</sub>-DMA were more similar to the straight-line curve and were inclined to nonionic polymers. This could have been due to the high cation/anion pairing and the absence of net charges along the chain, which lead to electrostatic repulsion.

Figure 4 shows the relation of the NaCl concentration to the reduced viscosity of the polyelectrolyte and polyampholyte at the IEP. The reduced viscosity of P-SO<sub>3</sub> decreased quickly with increasing NaCl concentration; this was a polyelectrolyte behavior. When the concentration of NaCl was about 0.4 mol/L, it began to deposit from the salt solution. The decreases in the hydrodynamic volume and coil twist (indicated by the decrease

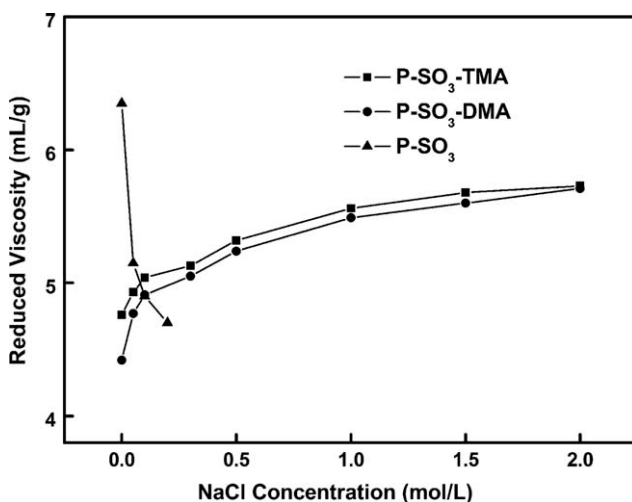


**Figure 4.** Effect of the NaCl concentration on the reduced viscosity of P-SO<sub>3</sub> at pH 2.5, P-SO<sub>3</sub>-TMA at pH 8.1 ( $\text{PH}_{\text{IEP}} = 4.08$ ), and P-SO<sub>3</sub>-DMA at pH 6.5 ( $\text{PH}_{\text{IEP}} = 3.84$ , polymer concentration = 0.01 g/mL).

in the reduced viscosity and deposition) were attributed to the shielding of electrostatic repulsion among the negative charges by the small-molecule electrolytes. Figure 4 shows a significantly increased reduced viscosity of P-SO<sub>3</sub>-TMA and P-SO<sub>3</sub>-DMA with increasing concentration of NaCl. Classical antipolyelectrolyte behaviors were exhibited by P-SO<sub>3</sub>-TMA and P-SO<sub>3</sub>-DMA. Because the number of cations and anions was equal, the electrostatic attractions existing between the internal and external molecules constrained the chain extension. In aqueous solution, the electrostatic attractions resulted in intramolecular aggregates among the intragroups and intrachains, a decrease in the hydrodynamic volume, and a closeness of conformation (indicated by a relatively low reduced viscosity). However, in aqueous salt solution, the electrostatic attractions among the groups were reduced by the screen of small electrolytes; this led to an increase in the hydrodynamic volume and expansion of the coil (indicated by the increase in reduced viscosity). In a comparison of the curves of P-SO<sub>3</sub>-TMA and P-SO<sub>3</sub>-DMA, the increased ratio of the reduced viscosity was almost similar to the increase of small electrolytes, although the reduced viscosity of P-SO<sub>3</sub>-DMA was lower than that of P-SO<sub>3</sub>-TMA, so it could reach the reduced viscosity of P-SO<sub>3</sub>-TMA at high concentrations. This may have been due to the large amount of small electrolytes with their strong shielding role. Because the influence of electrostatic attractions between the cation/anion charges and the hydrodynamic volume could be neglected, the close cation/anion pairing or loose cation/anion pairing did not matter. So the reduced viscosity of P-SO<sub>3</sub>-TMA and P-SO<sub>3</sub>-DMA could reach the same value.

**Influence of the Nature of Electrolytes on the Reduced Viscosity of the Polyampholyte.** The influence of various electrolytes having a common anion ( $\text{Cl}^-$ ) on the reduced viscosity of the polyampholyte can be seen from Figures 5 and 6. The ability of monovalent and divalent cationic charges influencing the conformations of the polyampholyte obeyed the following sequence:  $\text{NH}_4^+ < \text{Li}^+ < \text{Na}^+ < \text{K}^+$  for  $\text{NH}_4\text{Cl}$ ,  $\text{LiCl}$ ,  $\text{NaCl}$ , and  $\text{KCl}$  and  $\text{Mg}^{2+} < \text{Ca}^{2+}$  for  $\text{MgCl}_2$  and  $\text{CaCl}_2$ , respectively, which

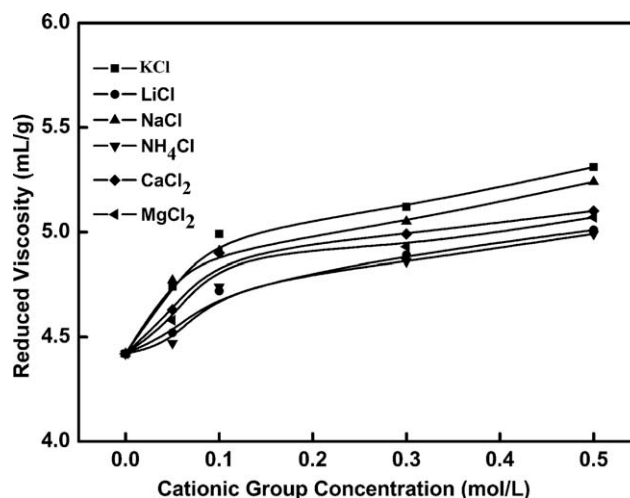


**Figure 5.** Effect of the cations on the reduced viscosity of P-SO<sub>3</sub>-DMA at pH 6.5 ( $\text{PH}_{\text{IEP}} = 3.84$ , polymer concentration = 0.01 g/mL).

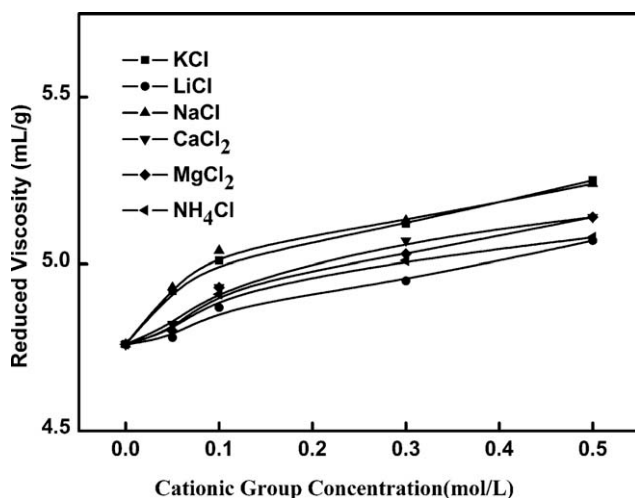


**Figure 6.** Effect of the cations on the reduced viscosity of P-SO<sub>3</sub>-TMA at pH 6.5 ( $P_{HIEP} = 4.08$ , polymer concentration = 0.01 g/mL).

were proven by the change range of the reduced viscosity. The result indicates that the cations with a small charge density were easily attracted to the sulfonate groups, and this led to a reduction of the electrostatic interactions between cations and anions. These tendencies conformed to the previous work.<sup>24,25</sup> So the residual cationic groups along the polymer chain exhibited electrostatic repulsion to extend the polymer chain.

The data of the reduced viscosity under the effect of various anions with a common cation ( $K^+$ ) are shown in Figures 7 and 8. The increase was in the order:  $Cl^- < Br^- < I^-$ . The result obtained confirmed the order of interaction of the anion with the quaternary ammonium group or tertiary amine group. This could be correlated to the polarizability increase of the anions from  $Cl^-$  to  $I^-$ . The anions with a small charge density were easily polarized as they approached and became bound to the quaternary ammonium groups or tertiary amine groups on the polymer unit. A similar tendency was also observed in the previous work.<sup>24,25</sup> So the reduced viscosity increased with

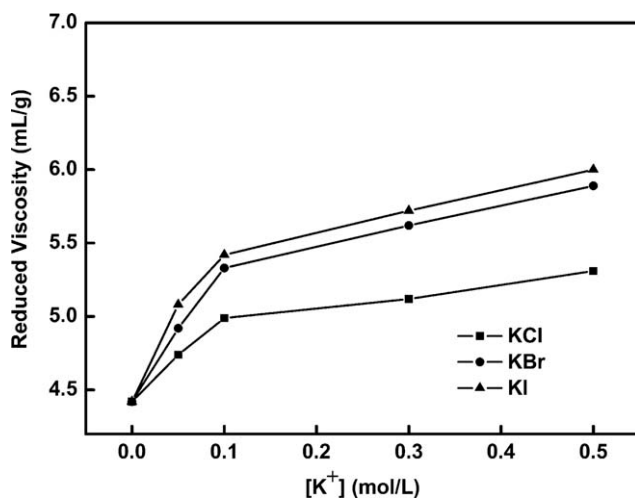


**Figure 7.** Effect of the anions on the reduced viscosity of P-SO<sub>3</sub>-DMA at pH 8.1 ( $P_{HIEP} = 3.84$ , polymer concentration = 0.01 g/mL).

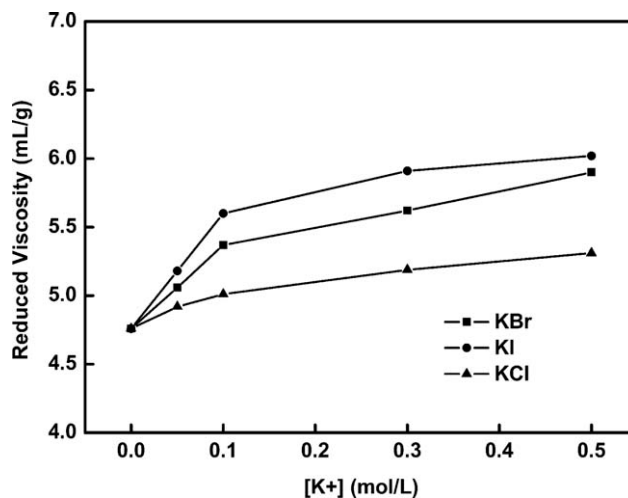


**Figure 8.** Effect of the anions on the reduced viscosity of P-SO<sub>3</sub>-TMA at pH 8.1 ( $P_{HIEP} = 4.08$ , polymer concentration = 0.01 g/mL).

increasing polarizability of the ions. Meanwhile, according to Pearson theory, the quaternary ammonium group (or tertiary amine group) and sulfonate group on the polymer unit could be considered as a soft acid and a soft base, respectively. Thus, soft bases (anions) from a salt (larger anionic radius) bonded more easily to sites on the quaternary ammonium group and tertiary amine group than hard bases, and soft acids (cations) from a salt (larger cationic radius) bonded more easily on the sulfonate group than hard acids.

It can be seen from the data in Table VI that the intrinsic viscosity was more sensitive to the nature of anions than that of cations. This could be attributed to the large hydration shell of the cations as a result of their large charge/radius ratio. Because of the large charge/radius ratio, it was difficult for them to approach close enough to effectively neutralize the charge on the sulfonic acid group. The anions were much more polarizable and had small hydration shells because of their small charge/radius ratio; hence, they were particularly effective in neutralizing the cationic ions along the polymer chain.

**Table VI.** Effect of the Anions and Cations on the Intrinsic Viscosity of P-SO<sub>3</sub>-TMA and P-SO<sub>3</sub>-DMA

Ion type	Intrinsic viscosity (mL/g)	
	P-SO <sub>3</sub> -TMA	P-SO <sub>3</sub> -DMA
KCl	5.81	5.81
KBr	6.39	6.39
KI	6.50	6.50
LiCl	5.57	5.51
NaCl	5.82	5.74
NH <sub>4</sub> Cl	5.58	5.49
CaCl <sub>2</sub>	5.64	5.60
MgCl <sub>2</sub>	5.64	5.57

P-SO<sub>3</sub>-TMA was measured at a pH of 8.1 with a concentration of 0.01 g/mL, whereas the P-SO<sub>3</sub>-DMA was measured at pH of 6.5 with a concentration of 0.01 g/mL.

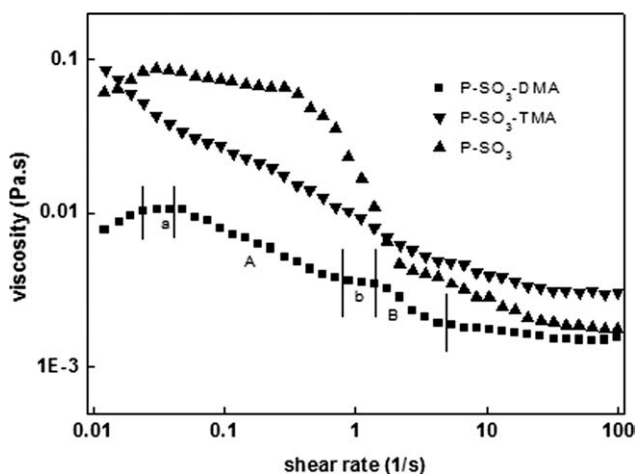


**Figure 9.** Viscosity of the P-SO<sub>3</sub>-TMA solution at pH 8.1 and P-SO<sub>3</sub>-DMA at pH 6.5 as a function of the shear rate in pure water (polymer concentration = 0.01 g/mL): (A) shear-thinning region 1, (B) shear-thinning region 2, (a) platform 1, and (b) platform 2.

**Viscosity of the Polymer Solutions on the Shear Rate.** Figure 9 represents the variations of the shear viscosity as a function of the shear rate for polyelectrolyte aqueous solutions and polyampholyte aqueous solutions. The rheological behavior of the solution of P-SO<sub>3</sub> showed a classical viscosity–shear rate curve at a low concentration and exhibited a low-shear Newtonian plateau followed by a smooth shear-thinning behavior at higher shear rates. Furthermore, the rheological curve of the solution of P-SO<sub>3</sub> showed a drastic shear-thinning region, which has been observed in previous work.<sup>40,41</sup> The viscosity of the polymer solution mainly relied on the conformation and space lattice structure of the polymer in the solution. So the rheological behavior of P-SO<sub>3</sub> could be attributed to the electrostatic repulsion in the space lattice structure. The chain of P-SO<sub>3</sub> exhibited a rodlike conformation because of the semirigidity of the backbone and electrostatic repulsion among the sulfonic acid groups along the chain. There was an equilibrium distance among the space lattice structures formed by the rodlike chain. At a low shear rate, the space lattice structure was compressed by shear stress, which made the distance less than the equilibrium distance ( $h$ ). As a result, the electrostatic repulsions restrained the compression and maintained the stability of space lattice structure. When the shear rate reached a critical value, the shear stress could resist electrostatic repulsions to disrupt the space lattice structure, and the drastic shear-thinning region was observed. Furthermore, when the structure was disrupted, it was difficult to form a new structure because of the electrostatic repulsion among the chains. So the viscosity decreased sharply to the lowest value in the solution.

As shown in Figure 9, the rheological behavior of the solution of P-SO<sub>3</sub>-TMA exhibited a shear-thinning region and a higher viscosity retention compared to that of P-SO<sub>3</sub>. Because of the cationic and anionic ions along the polymer chain, there were electrostatic attractions both in the intramolecular and intermolecular directions. Furthermore, the electrostatic attractions were weak because of the loose ion pair aroused by quaternary

ammonium and sulfonic acid groups of the strong ionization. So at the low shear rate, such as below 0.1 s<sup>-1</sup>, the viscosities decreased; this could be attributed to the weak force needed to maintain the space lattice structure in the solution. Although the space structure was easily disrupted, new structures among the polymer chains were also easily formed because of the electrostatic attraction. In other words, the disruption and formation of space structure coexisted; this led to a gradual decrease of the viscosity versus shear rate. At a high shear rate, when the space lattice structure was completely disrupted, the balance viscosity of P-SO<sub>3</sub>-TMA was still higher than that of P-SO<sub>3</sub>; this could be attributed to the electrostatic attraction among the polymer chain.

The rheological curve of the solution of P-SO<sub>3</sub>-DMA showed two shear-thinning regions and two platform regions in Figure 9. The strong nonlinear behavior, because of the discontinuities of the curve of viscosity versus shear rate, has been observed by the previous work.<sup>40–42</sup> In the first platform region, a classical flow curve at a low shear rate, which is called a low-shear Newtonian plateau, existed. This could be explained by the strong electrostatic attraction compared to that of P-SO<sub>3</sub>-TMA, which was aroused by the close ion pair between sulfonic acid groups of strong ionization and tertiary amine groups of weak ionization. The strong electrostatic attraction could maintain the stability of the space lattice structure in the aqueous solution. So the first platform region could be attributed to the strong extramolecular attraction, which could maintain the stability of the space lattice structure. It is worth noticing that the second drastic shear-thinning region, and the intermediate plateau (i.e., the region between the two abrupt shear-thinning regimes) were more or less marked according to the polymeric system. The second platform region could be attributed to the dynamic equilibrium of the space lattice structure formation, and the dynamic equilibrium was maintained by electrostatic attraction and the destruction of shear stress. However, at a much higher shear rate, the space lattice structure was absolutely destroyed by the overwhelming shear stress. The viscosity of the solution

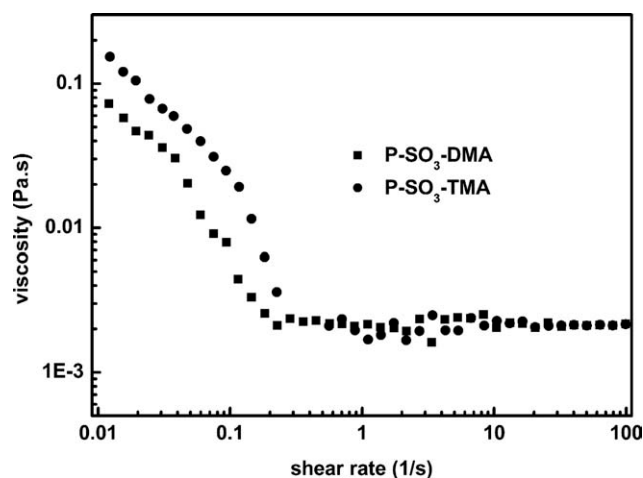


**Figure 10.** Viscosity curves of the P-SO<sub>3</sub>-TMA solution at pH 8.15 and P-SO<sub>3</sub>-DMA at pH 6.46 in saturated salt water (polymer concentration = 0.01 g/mL).



of P—SO<sub>3</sub>—DMA gradually kept a constant value. Furthermore, because of the strong force between the cationic and anionic ions, the strong extramolecular attraction ultimately led to a much lower viscosity in the solution of P—SO<sub>3</sub>—DMA than in the solution of P—SO<sub>3</sub>—TMA.

Figure 10 represents the rheological behaviors of P—SO<sub>3</sub>—DMA and P—SO<sub>3</sub>—TMA in saturated salt water.

It was observed that with increasing shear rate, the viscosity decreased quickly to reach a platform. This could be attributed to the screen of small electrolytes to the cationic/anionic ions, which led to electrostatic interaction to maintain the space lattice structure in the aqueous solution.<sup>43</sup>

## CONCLUSIONS

A convenient and effective route for obtaining polyelectrolytes and polyampholytes has been described in this article. Through the postsulfonation of PPS, a kind of polyelectrolyte was prepared. Through bromination and then the substitution of bromine by a quaternary ammonium group and tertiary amine group of P—SO<sub>3</sub>, the polyampholyte was obtained. The solution properties of the polyelectrolyte and polyampholyte were controlled by electrostatic interactions of different group types, such as sulfonic groups, quaternary ammonium groups, and tertiary ammonium groups, and extra factors, such as the pH, small electrolytes, and concentration. The antipolyelectrolyte effect of the polyampholyte was observed in this study. The rheological behavior of the polyelectrolyte in pure water was investigated by with a Malvern Gemini rheometer. The rheological behaviors of the polyampholyte in pure water and saturated salt water were also investigated with the Malvern Gemini rheometer. A critical shear rate was observed for the polyelectrolyte in pure water. The rheological behaviors of the polyampholyte showed relatively stability of the shear rate compared to the polyelectrolyte in pure water. However, in saturated salt water, the viscosity of the polyampholyte decreased quickly with increasing shear rate.

## REFERENCES

1. Kudaibergenov, S. E. *Adv Polym Sci* **1999**, *114*, 115.
2. Andrew, B. L.; Charles, L. M. *Chem Rev* **2002**, *102*, 4177.
3. Ryan, G. E.; Charles, L. M. *J Appl Polym Sci* **2007**, *104*, 2812.
4. Xuan, F. Q.; Liu, J. S. *Polym Int* **2009**, *58*, 1350.
5. Andrey, V. D.; Micheal, R. *J Phys II Fr* **1995**, *5*, 677.
6. Dobrynin, A. V.; Colby, R. H.; Rubinstein, M. *J Polym Sci Part B: Polym Phys* **2004**, *42*, 3513.
7. Ibraeva, Z. E.; Hahn, M.; Jaeger, W.; Bimendina, L. A.; Kudaibergenov, S. E. *Macromol Chem Phys* **2004**, *205*, 2464.
8. Alfrey, T. J.; Morawetz, H.; Fitzgerald, E. B.; Fuoss, R. M. *J Am Chem Soc* **1950**, *72*, 1864.
9. Das, M.; Kumacheva, E. *Colloid Polym Sci* **2006**, *284*, 1073.
10. Yang, J. H.; John, M. S. *J Polym Sci Part A: Polym Chem* **1995**, *33*, 2613.
11. Zheng, G. Z.; Meshitsuka, G.; Ishizu, A. *J Polym Sci Part B: Polym Phys* **1995**, *33*, 867.
12. Xu, S.; Cao, L.; Wu, R.; Wang, J. *J Appl Polym Sci* **2006**, *101*, 1995.
13. Baker, J. P.; Blanch, H. W.; Prausnitz, J. M. *Polymer* **1995**, *36*, 1061.
14. Kudaibergenov, S.; Jaeger, W.; Laschewsky, A. *Adv Polym Sci* **2006**, *201*, 157.
15. Yuan, J.; Zhu, J.; Zhu, C. H.; Shen, J.; Lin, S. C. *Polym Int* **2004**, *53*, 1722.
16. Zhang, L. M.; Tan, Y. B.; Li, Z. M. *Carbohydr Polym* **2001**, *44*, 255.
17. Zhang, L. M.; Chen, D. Q. *Macromol Mater Eng* **2003**, *288*, 252.
18. Zhang, L. M.; Tan, Y. B.; Li, Z. M. *Colloid Polym Sci* **1999**, *277*, 1001.
19. Zhang, J.; Zhang, L. M.; Li, Z. M. *J Appl Polym Sci* **2000**, *78*, 537.
20. Bruton, J. R.; McLaurine, H. C. Presented at Soc Plast Eng Annual Technical Conference and Exhibition, Oct **1993**, Houston, Texas; SPE26327.
21. Peiffer, D. G.; Xiao, H.; Tao, R.; Cui, W.; Zhang, S.; Li, R. U.S. Pat. 4,626,285 (**1986**).
22. Fevola, M. J.; Bridges, J. K.; Kellum, M. G.; Hester, R. D.; McCormick, C. L. *J Appl Polym Sci* **2004**, *94*, 24.
23. Nelly, B.; Andren, L. *Polymer* **1996**, *10*, 2011.
24. Ali, S. A.; Rasheed, A. *Polymer* **1999**, *40*, 6849.
25. Lee, W.-F.; Huang, G.-Y. *Polymer* **1996**, *37*, 4389.
26. Zheng, Z.; Timothy, C.; Sheng, F. C.; Shao, Y. J. *Langmuir* **2006**, *22*, 10072.
27. Kudaibergenov, S. F.; Ciferri, A. *Macromol Rapid Commun* **2007**, *28*, 1969.
28. Kudaibergenov, S.; Jaeger, W.; Laschewsky, A. *Adv Polym Sci* **2006**, *201*, 157.
29. Yin, Q.; Li, Y.; Yin, Q.-J.; Miao, X.; Jiang, B. *J Appl Polym Sci* **2009**, *113*, 3382.
30. Souguir, Z.; Roudesli, S.; About-Jaudet, E.; Cerf, D. L.; Piction, L. *J Colloid Interface Sci* **2007**, *313*, 108.
31. Nikoletta, S.; Thierry, A.; Constantinos, T. *Polymer* **2008**, *49*, 1249.
32. Frederic, B.; Vasiliki, S.; Constantinos, T. *Macromolecules* **2004**, *37*, 3899.
33. Matthew, G.; McKee, M. T.; et al. *Macromolecules* **2006**, *39*, 575.
34. Cheng, X. X.; Zhang, X. F.; Liu, J. S.; Xu, T. W. *Eur Polym J* **2008**, *44*, 918.
35. Shibuya, N.; Roger, S. *Macromolecules* **1992**, *25*, 6495.
36. Lufrano, F.; Squadrito, G.; Patti, Q.; Passalacqua, E. *J Appl Polym Sci* **2000**, *77*, 1250.
37. Jia, X.; Zhang, Y. J. *J Appl Polym Sci* **2010**, *118*, 1152.
38. Ye, L.; Huang, R.; Wu, J.; Hoffmann, H. *Colloid Polym Sci* **2004**, *282*, 305.
39. Andrew, B.; Lowe, Charles, L. *Chem Rev* **2002**, *102*, 4177.
40. Stavrouli, N.; Aubry, T.; Tsitsilianis, C. *Polymer* **2008**, *49*, 1249.
41. Berret, J. F.; Serero, Y.; Winkelmann, B.; Calvet, D.; Collet, A.; Viguier, M. *J Rheol* **2001**, *45*, 477.
42. Berret, J. F.; Serero, Y. *Phys Rev Lett* **2001**, *87*, 483031.
43. Xie, G.; Li, Y.; Chen, J. S. *Chin J Appl Chem* **2002**, *17*, 72.